



# Near-continuous isotropic – nematic transition in compressed rod-like liquid crystal based nanocolloid

Joanna Łoś<sup>a,\*</sup>, Aleksandra Drozd-Rzoska<sup>a,\*</sup>, Sylwester J. Rzoska<sup>a</sup>, Szymon Starzonek<sup>d</sup>, Krzysztof Czupryński<sup>b</sup>, Prabir Mukherjee<sup>c</sup>

<sup>a</sup> Institute of High Pressure Physics Polish Academy of Sciences, ul. Sokolowska 29/37, 01-142 Warsaw, Poland

<sup>b</sup> Military University of Technology, Faculty of Advanced Technologies and Chemistry, ul. gen. Sylwestra Kaliskiego 2, 00-908 Warsaw, Poland

<sup>c</sup> Department of Physics, Government College of Engineering and Textile Technology, 12 William Carey Road, Serampore, Hooghly 712201, India

<sup>d</sup> Laboratory of Physics, Faculty of Electrical Engineering, University of Ljubljana, Tržaška 25, 1000 Ljubljana, Slovenia

## ARTICLE INFO

### Keywords:

Liquid crystals  
Nanocolloids  
High pressures  
I-N transition  
Critical phenomena  
Dynamics  
Broadband dielectric spectroscopy

## ABSTRACT

Landau-de Gennes mean-field model predicts the discontinuous transition for the isotropic – nematic (I-N) transition, associated with uniaxial ordering and a quadrupolar order parameter in three dimensions. This report shows pressure-related dielectric studies for rod-like nematogenic pentylcyanobiphenyl (5CB) and its nanocolloids with BaTiO<sub>3</sub> nanoparticles. The scan of the dielectric constant revealed the near-continuous I-N phase transition in the compressed nanocolloid with a tiny amount of nanoparticles ( $x = 0.1\%$ ).

For the nematic phase in 5CB and its  $x = 1\%$  nanocolloid the enormous values of the dielectric constant and the bending-type, long-range pretransitional behavior were detected. The impact of prenematic fluctuations was also noted for the ionic-related contribution to dielectric permittivity in the isotropic liquid phase. For the high-frequency relaxation domain, this impact was tested for the primary relaxation time pressure evolution and the translational–orientational decoupling.

## 1. Introduction

The phase transition from the isotropic liquid (I) to the nematic phase (N) in rod-like liquid crystalline materials can be considered an example of a challenging fluid–fluid transition phenomenon [1–3]. It is also the atypical freezing/melting weakly discontinuous phase transition, where the process is associated with a single element of symmetry – the uniaxial arrangement. The I-N transition also means entering the ‘intermediate’ state of matter, liquid crystal (LC), which combine fluidity with a limited crystalline ordering. Particularly worth stressing is the ‘weakness’ of the I-N phase transition discontinuity [4–6]. For instance, in such classic LC material as pentylcyanobiphenyl (5CB) the entropy changes at the I-N transition are  $\Delta S \approx 8JK^{-1}kg^{-1}$ , whereas  $\Delta S \approx 160JK^{-1}kg^{-1}$  for the nematic – solid (N-S) transition [7,8].

The hallmarks of the I-N transition, absent for canonic melting/freezing, are long-range pretransitional effects associated with critical-like prenematic fluctuations in the isotropic liquid phase [4–6]. Their significance was discovered by Pierre Gilles de Gennes [9,10] who noted

the simple ‘universal’ temperature changes of the Cotton Mouton effect (CME,  $\Delta n/\lambda H^2$ ) and Rayleigh light scattering ( $I_L$ ) in the isotropic liquid phase. Later similar behavior was also observed for the Kerr effect (KE,  $\Delta n/\lambda E^2$ ), nonlinear dielectric effect (NDE,  $\Delta \epsilon/E^2$ ) and compressibility ( $\chi_T$ ). All these magnitudes follow the same simple scaling pattern [4,6,9–20]:

$$\frac{\Delta n}{\lambda H^2}, \frac{\Delta n}{\lambda E^2}, \frac{\Delta \epsilon}{E^2}, I_L, \chi_T = \frac{m}{T - T^*} \quad (1a)$$

$$\left(\frac{\Delta n}{\lambda H^2}\right)^{-1}, \left(\frac{\Delta n}{\lambda E^2}\right)^{-1}, \left(\frac{\Delta \epsilon}{E^2}\right)^{-1}, (I_L)^{-1}, \chi_T^{-1} = mT - mT^* \quad (1b)$$

where  $m$  denotes the amplitude related to the given method,  $\Delta n$  is the magnetic ( $H$ ) or electric ( $E$ ) field induced birefringence,  $\lambda$  denotes the applied light wavelength,  $\Delta \epsilon = \epsilon - \epsilon(E)$  are electric field induced changes of dielectric constant,  $T > T_{I-N}$  and  $T^* = T_{I-N} - \Delta T^*$ , the latter is the temperature metric for the I-N transition discontinuity.

De Gennes [9,10] linked the Landau phenomenological model [21],

\* Corresponding authors.

E-mail addresses: [joalos@unipress.waw.pl](mailto:joalos@unipress.waw.pl) (J. Łoś), [Ola.DrozdRzoska@gmail.com](mailto:Ola.DrozdRzoska@gmail.com) (A. Drozd-Rzoska), [sylwester.rzoska@gmail.com](mailto:sylwester.rzoska@gmail.com) (S.J. Rzoska), [Szymon.starzonek@fe.uni-lj.si](mailto:Szymon.starzonek@fe.uni-lj.si) (S. Starzonek), [krzysztof.czuprynski@wat.edu.pl](mailto:krzysztof.czuprynski@wat.edu.pl) (K. Czupryński), [pkmuk1966@gmail.com](mailto:pkmuk1966@gmail.com) (P. Mukherjee).

<https://doi.org/10.1016/j.molliq.2023.121844>

Received 8 November 2022; Received in revised form 14 March 2023; Accepted 12 April 2023

Available online 18 April 2023

0167-7322/© 2023 Elsevier B.V. All rights reserved.

considering near-critical free energy  $F$  via the order parameter power series expansion, with the nematic order parameter definition introduced by Tsvetkov [22,23]. It led to the following relation [9,10,24]:

$$F = F_0 + aQ_{\alpha\beta}Q_{\beta\alpha} - bQ_{\alpha\beta}Q_{\beta\gamma}Q_{\gamma\alpha} + c(Q_{\alpha\beta}Q_{\beta\alpha})^2 - G(H_\alpha H_\beta, E_\alpha E_\beta) \quad (2)$$

where  $Q_{\alpha\beta} = \frac{1}{2}S(3n_\alpha n_\beta - \delta_{\alpha\beta})$  is the quadrupolar order parameter reflecting the equivalence of  $\vec{n}$  and  $-\vec{n}$  directors indicating the preferred uniaxial ordering of rod-like molecules [22,23];  $b$ ,  $c$ ,  $G$  are constant amplitudes [9,10,24]. In the isotropic phase:  $a = a_0(T - T^*)$ , and  $T^*$  is the extrapolated hypothetical continuous (critical) phase transition. The last term in Eq. (2) reflects the impact of the magnetic (H) or electric (E) field.

Substituting  $Q_{\alpha\beta}$  order parameter to Eq. (2) one obtains [4,6,24]:

$$F = F_0 + \frac{3}{2}aS^2 - \frac{3}{4}bS^3 + \frac{9}{4}cS^4 - \dots G(H^2, E^2) \quad (3)$$

According to critical phenomena physics [4], for which critical exponents are essential universal parameters, the basic Landau – de Gennes (LdG) model yields:  $\gamma = 1$  for the compressibility-related exponent, as in Eq. (1), and  $\beta = 1/2$  for the order parameter exponent in the nematic phase. For such basic magnitude as the specific heat exponents  $\alpha = 1/2$  in the nematic phase and  $\alpha = 0$  in the isotropic liquid phase in the mean field approximation are expected [4,25-28]. The latter is in explicit disagreement with extensive experimental evidence showing  $\alpha = 1/2$  for both sides of  $T_{I-N}$  [4,6,29]. The agreement with the experiment appears when considering I-N transition as the near-tricritical point (TCP) case. TCP-related pretransitional behavior is associated with the following values of exponents:  $\alpha = 1/2, \gamma = 1$  and  $\beta = 1/4$  [4,29,30]. Notwithstanding the exponent  $\alpha = 1/2$  can also appear in the basic mean field LdG model when corrections considering the density changes linked to fluctuations are included [31]. The experimental evidence regarding the order parameter exponent is split. There is a set of reliable experimental results yielding  $\beta = 1/2$  in agreement with the basic mean-field LdG model approach [4,24,32-34]. On the other hand, the distortions-sensitive analysis reduced the number of fitted parameters and yielded  $\beta = 1/4$  in heptyloxycyanobiphenyl (6OCB) [35], octyloxycyanobiphenyl (8OCB) [36], and 5CB [37].

When discussing properties of rod-like LC materials, the importance of dielectric studies associated with the extreme sensitivity to the electric field is worth stressing. This feature is the base of numerous applications in displays and photonic devices [38] and strongly shaped the fundamental insight [4,6,32]. The in-deep knowledge regarding dielectric constant changes is particularly important for both areas. Generally, on approaching a critical point in liquids, the following link between the behavior of specific heat (or heat capacity) and dielectric constant was suggested theoretically:  $c_v(T) = d\varepsilon(T)/dT$  [39,40]. This prediction inspired the development of the relation describing pretransitional changes of dielectric constant in the isotropic liquid phase on approaching I-N transition [36,37,41,42]:

$$\varepsilon(T) = \varepsilon^* + a_\varepsilon(T - T^*) + A_\varepsilon(T - T^*)^{1-\alpha} \quad (4)$$

Generally, three important fundamental issues have to be stressed when discussing I-N transition. First, Landau - de Gennes (LdG) mean-field model predicts the discontinuous transition for the isotropic – nematic (I-N) transition, associated with uniaxial ordering and a quadrupolar order parameter in three dimensions [4,9,10]. Consequently, a common consensus exists for the generic discontinuity for I-N transition in rod-like systems [4,6,24,29,32]. We omit here the quasi-continuous case when the phase transition is stretched in some temperature domains [43-46]. Second, rod-like LC systems can serve as a unique ‘experimental model’ facilitating the theoretical and simulation insights into the still challenging glassy dynamics domain [47-51]. Third, LC systems are enormously sensitive to endogenic and exogenic impacts, such as pressure [17,37] and the addition of nanoparticles (NPs) [50-

53], for instance. The latter recalls the new research area of LC-based nanocolloids and nanocomposites, which have enormously developed in the last decades. It is related to emerging unique fundamental properties of such systems, but the key motivator constitutes possibilities of applications in innovative photonic devices [52-54].

There are still significant cognitive gaps in studies on LC + NPs nanocolloids, namely: (i) the limited evidence regarding the impact of pretransitional fluctuations essential in basic LC compounds and (ii) the practical lack of pressure-related studies in LC-based nanocolloids.

This report presents high-pressure studies of 5CB and its nanocolloids with BaTiO<sub>3</sub> nanoparticles, focused on the impact of pretransitional fluctuations and the emergence of complex, glassy-type dynamics. Amongst the results obtained worth stressing is the evidence for the near-continuous I-N transition emerging in compressed 5CB + NPs nanocolloid.

The latter recalls the fundamental question regarding the existence or non-existence of the liquid–crystal critical point, posed by Lev. D. Landau.

## 2. Experimental

Studies were carried out in 4-pentyl-4'-cyanobiphenyl (pentylcyanobiphenyl, 5CB), the rod-like liquid crystalline (LC) compound, with the following mesomorphism [32]:

*Crystal* ← 288.0K ← *Nematic* ← 308.2K ← *Isotropic*. 5CB belongs to the most frequently investigated LC compounds regarding both applications and fundamental research. 5CB molecule has a rod-like shape, with a permanent dipole moment approximately parallel to the long molecular axis:  $\mu = 5.95 D$  [32]. The compound was synthesized at the Military University of Technology (Poland), by Krzysztof Czupryński team, which also deeply cleaned samples to reduce contaminations to minimize a parasitic rise in electric conductivity. It was also degassed immediately before measurements which also additionally cleaned samples. Paraelectric BaTiO<sub>3</sub> nanopowder (diameter  $d = 50$  nm) was purchased from US Research Nanomaterials, Inc. [55]. Mixtures of liquid crystal and nanoparticles were sonicated at a temperature higher than the isotropic to nematic phase transition for 4 h to obtain homogeneous suspensions. Studies were carried out for 5CB + 0.1% and 5CB + 1% of BaTiO<sub>3</sub> nanoparticles. Such selection was motivated by two facts. First, our experience shows that for concentration above 1% a sedimentation of nanoparticles can occur. One can avoid it introducing a macromolecular surface agent, but it significantly distorts dielectric response and can yield a shift of the clearing temperature. Regarding the lowest (0.1%) tested concentration of nanoparticles, it was motivated by earlier studies in nematogenic 5OCB under atmospheric pressure, where the addition of 0.1% BaTiO<sub>3</sub> caused an extraordinary decrease of discontinuity to  $\Delta T^* \approx 0.3K$  [56]. We stress that preparing nanocolloids with so few nanoparticles is always troublesome for the laboratory. It requires a large amount of expensive (high purity class) liquid crystalline material. Paraelectric properties and the globular form of nanoparticles (NPs) enabled the minimization of their phase- and shape-related orientational impact on the host LC system. Concentrations of nanoparticles (NPs) are given in weight fraction percentage (wt%).

Tested samples were placed in a flat-parallel capacitor (diameter  $2r = 10$  mm), made of Invar. The distance between plates:  $d = 0.15$  mm. The capacitor was based on the design shown in ref. [57], which enables reliable isolation from the pressure-transmitting medium (Plexol), which always constitutes a challenge in high-pressure studies. The high-pressure chamber system was designed by Unipress Equipment.

The body of the pressure chamber was surrounded by a jacket, enabling the circulation of a liquid from the large volume ( $V = 20$  L) Julabo thermostat. The temperature was measured inside the chamber using a copper – constantan thermocouple ( $\pm 0.02$  K) and two Pt100 resistors placed in the body of the chamber, to test possible temperature gradients. Changes in pressure were created via the computer-controlled

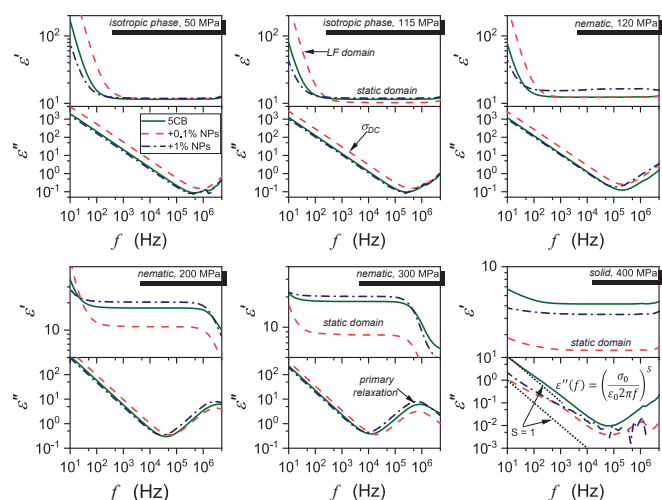


**Fig. 1.** Examples of BDS spectra—the real ( $\epsilon'$ ) and imaginary ( $\epsilon''$ ) parts of dielectric permittivity as a function of frequency collected for 5CB and its nanocolloids under pressure. Significant features and domains are indicated. They are the low-frequency (LF) domain, the static domain associated with the dielectric constant, the primary loss curve, and the frequency part used for determining DC electric conductivity. Results for isothermal ( $T = 353\text{K}$ ) compressing.

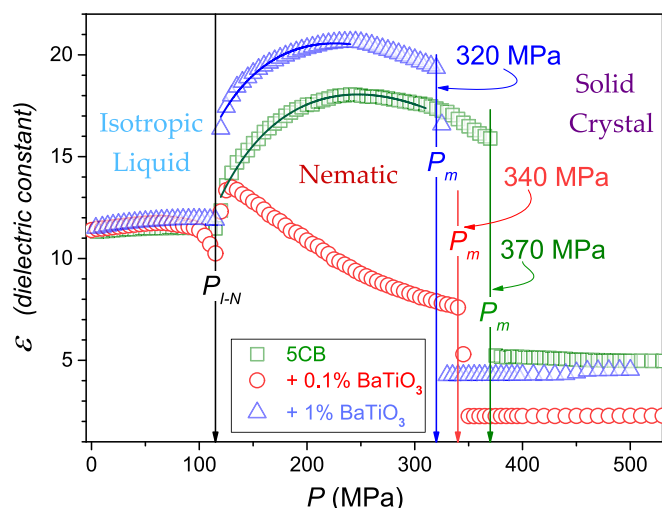


**Fig. 2.** Isothermal, pressure evolutions of dielectric constant in compressed 5CB and its nanocolloids with  $\text{BaTiO}_3$  nanoparticles on compressing, for  $T = 353\text{ K}$  isotherm. The vertical arrows indicate the I-N transition pressure ( $P_{I-N}$ ) and melting pressures ( $P_m$ ) for Nematic to Crystal transitions, in colors linked to given concentrations of nanoparticles. Solid curves in the nematic phase are related to Eq. (11).

pressure pump and measured using the tensometric pressure meter ( $\pm 0.2\text{ MPa}$ ).

Broadband dielectric spectroscopy (BDS) studies were carried out using a Novocontrol Alpha-A analyzer in the frequency range from 1 Hz to 10 MHz, enabling 5–6 digits permanent resolution for tested complex dielectric permittivity spectra. Up to 140 spectra were detected in the tested range of pressures, extending up to  $P = 0.6\text{--}0.8\text{ GPa}$ . This range was associated with essential problems in BDS studies for higher frequencies. The voltage of the measuring field  $U = 1\text{ V}$  was applied. Examples of dielectric permittivity spectra are shown in Fig. 1. It also presents significant features of such spectra. As the reference frequency for the dielectric constant  $\epsilon = \epsilon'(f = 116\text{ kHz})$ , in the static domain, was chosen. The primary relaxation time was determined from the peak of

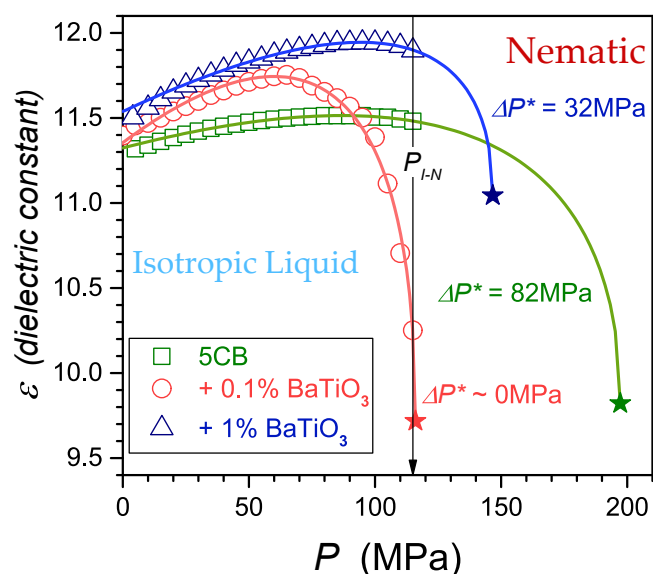


**Fig. 3.** The detailed insight into the pretransitional behavior of dielectric constant in the isotropic liquid phase of 5CB and its nanocolloids with  $\text{BaTiO}_3$  nanoparticles for the pressure-related approach to the I-N transition. Solid curves are related to Eq. (5) with parameters given in Table 1. Stars denote the hypothetical extrapolated phase transition. The I-N phase transition pressure detected in experiments is marked with a vertical arrow.

the primary loss curve in the high-frequency part of  $\epsilon''(f)$  spectrum as  $\tau = 1/2\pi f_{\text{peak}}$ , and DC electric conductivity from its low-frequency (LF) part:  $\sigma = 2\pi f \epsilon_0 \epsilon''(f)$ , where  $\epsilon_0$  is the vacuum permittivity [5,58]. The latter relation ceases to obey in the solid phase for 5CB +  $\text{BaTiO}_3$  nanocolloids under compressing, as shown in Fig. 2.

The stability of nanocolloidal samples was tested by measuring the dielectric constant and electric conductivity in a special capacitor with rectangular plates: 20 mm in length and 5 mm in width, with two sections. Tests were conducted in the isotropic liquid and the nematic phase to the ‘longitudinal’ and ‘transverse’ positions. No changes in dielectric properties were noted during the high 5 h of observations. Notable, that high-pressure conditions increase density and viscosity, which additionally positively affects the stability of the system. Additional direct under-compressing observations were also made using the polarized light microscope. No signs of sample decomposition were observed.

The report contains three Appendixes, presenting and discussing significant supplementary issues: (1) is for the pressure evolution of the I-N temperature, showing also the applied in this report path of studies, (2) presents the temperature-related background of the relation describing the pressure evolution of the ‘parallel’ component of dielectric constant in the nematic phase, and (3) presents polarization microscopy photos for 5CB and 5CB +  $\text{BaTiO}_3$  nanocolloids on compressing, up to almost 0.5 GPa.

### 3. Results and discussion

Fig. 2 shows pressure evolutions of dielectric constant in 5CB and tested nanocolloids, covering isotropic (I), nematic (N), and solid crystal (S, Cr) phases. Studies are related to the isothermal path, shown in Appendix 1, where  $T_{I-N}(P)$  dependence in pure 5CB is presented. The lack of the influence of nanoparticles addition on  $P_{I-N}$ , visible in Fig. 2, suggests that such evolution of  $T_{I-N}(P)$  is preserved for nanocolloids discussed in the given report.

Fig. 3 presents a focused insight into the pretransitional behavior in the isotropic liquid phase. Pretransitional changes of dielectric constant can be portrayed by the pressure counterpart of Eq. (4) [5,37,40]:

$$\epsilon(P) = \epsilon^* + a_P(P^* - P) + A_P(P^* - P)^{1-\alpha}, T = \text{const} \quad (5)$$

**Table 1**

Values of parameters describing pressure-related pretransitional changes of dielectric constant (Eq. (5) and Fig. 3) in the isotropic phase of 5CB and its nanocolloids. Errors of presented value are related to the last number in given values.

Parameter	5CB	+ 0.1% NP	+ 1% NP
$\epsilon_{I-N}$	11.48	10.25	11.90
$P_{I-N}$ (MPa)	115	115	115
$a_p$	-0.02	-0.04	-0.02
$A_p$	0.32	0.54	0.25
$\alpha$	0.5	0.5	0.5
$\epsilon^*$	9.82	9.72	11.04
$P^*$ (MPa)	197	116	147
$\Delta P^*$ (MPa)	82	1	32

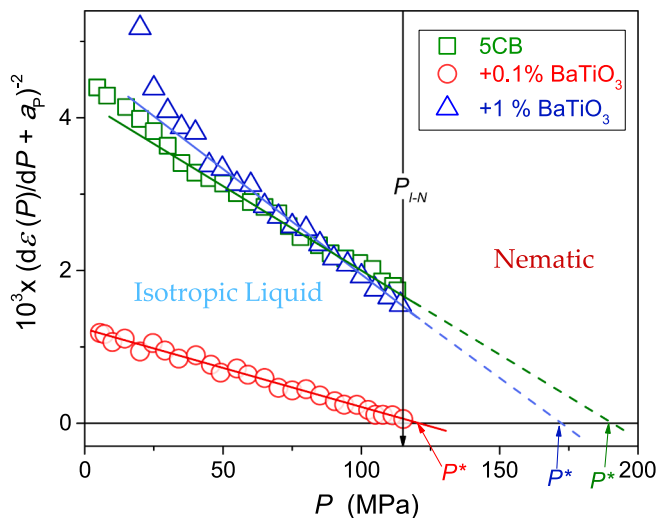


**Fig. 4.** The derivative-based plot showing results of the transformation of  $\epsilon(P)$  experimental data via Eq. (9), in the isotropic phase of 5CB and its nanocolloids. The appearance of the linear behavior validates the portrayal of  $\epsilon(P)$  pretransitional changes via Eq. (5), with the critical exponent  $\alpha = 1/2$ . The dashed lines are the extrapolations into the nematic phase. Hypothetical continuous phase transitions related to singular pressures  $P^*$  are indicated.

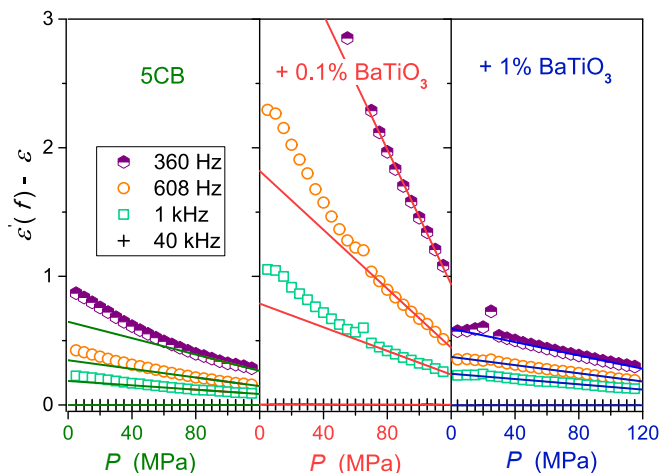


**Fig. 5.** Pressure evolutions of the ionic contribution to the dielectric constant (Eq. (11)) in the isotropic liquid phase of 5CB and its nanocolloids.

where  $(P^*, \epsilon^*)$  are coordinates of the extrapolated hypothetical continuous I-N transition,  $P < P_{I-N} = P^* - \Delta P^*$ , and  $\Delta P^*$  is the pressure metric of the I-N phase transition discontinuity;  $a_p$  and  $A_p$  are constant am-

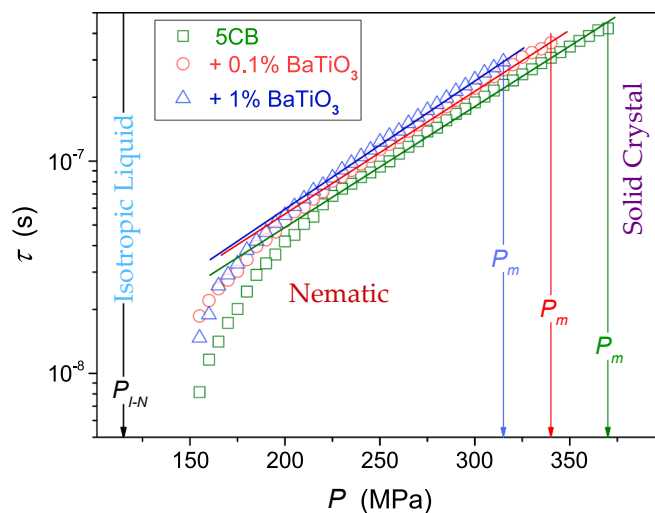


**Fig. 6.** Changes of the primary relaxation time in the nematic phase of 5CB and its nanocolloids with BaTiO<sub>3</sub> nanoparticles on compressing for  $T = 353$  K isotherms. The applied scale facilitates showing the basic Barus relation, as linear dependences. The limited frequency range in high-pressure studies enabled tests of basic properties characterizing dynamics only in the nematic phase.

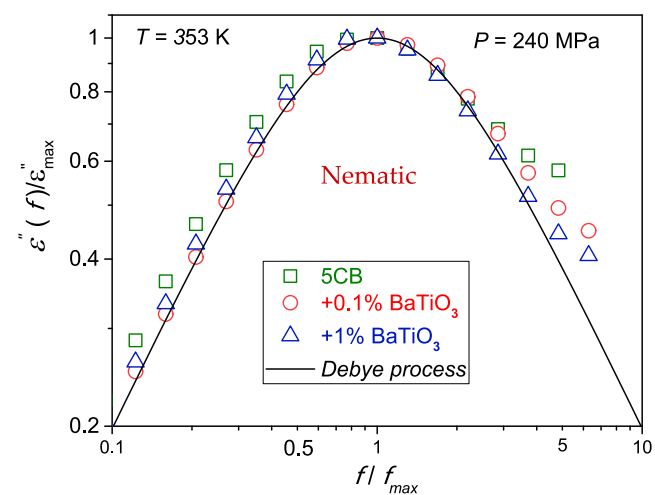


**Fig. 7.** The normalized superposition of dielectric loss curves in the mid of the nematic phase reached due to compressing 5CB and its nanocolloids with BaTiO<sub>3</sub> nanoparticles.

plitudes. The results of fitting Eq. (5) to data in the isotropic liquid phase are collected in Table 1.

The similarity between the isobaric, temperature-related Eq. (4) and the isothermal pressure-related Eq. (5), with the same value of the critical exponent  $\alpha$ , agrees with the Isomorphism Postulate for Critical Phenomena [4], and earlier dielectric studies of pretransitional effects in critical liquids [5,17,37,40,59-63].

Notable that the pretransitional anomaly described by Eq. (4) is associated with the crossover:

$$d\epsilon(T)/dT < 0 \leftarrow d\epsilon(T)/dT > 0 \text{ for } P = \text{const} \quad (6)$$

It is associated with permanent dipole moments ordered in an anti-parallel way within prenematic fluctuations, which leads to the cancellation of the dipolar contribution to the dielectric constant.

Consequently, the dielectric constant related to fluctuations is significantly lower than for their isotropic liquid surrounding. Near the I-N transition, the volume occupied by prenematic fluctuations dominates, yielding the above crossover. A similar crossover pattern appears

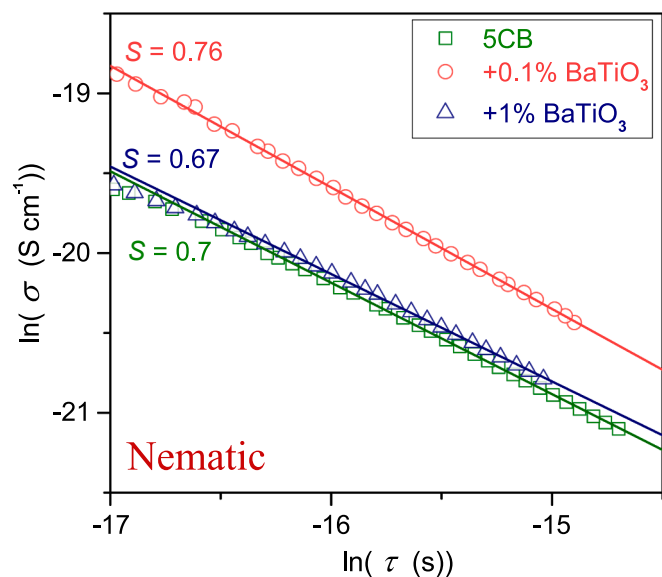


Fig. 8. Test of the translational-orientational decoupling in the nematic phase of compressed 5CB and its nanocolloids with BaTiO<sub>3</sub>.

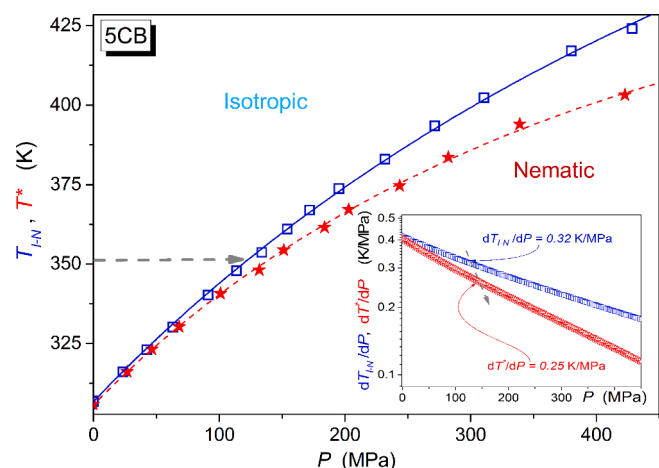


Fig. A1. Pressure dependence of the I-N clearing temperature ( $T_{I-N}$ ) and the extrapolated temperature of a continuous phase transition ( $T^*$ ). The latter was obtained using low-frequency nonlinear dielectric effect measurements. The parameterization is based on Eq. (A1.1). The inset shows pressure related changes  $dT_{I-N}/dP$  and  $dT^*/dP$  as a function of pressure resulted from such parameterization. The horizontal arrow in the main plot is related to the applied path of studies. In the inset values related to given tests are indicated. The plot was prepared based on the authors' data from ref. [78].

on compressing towards the I-N transition:

$$d\epsilon(P)/dP > 0 \rightarrow d\epsilon(P)/dP < 0 \text{ for } T = \text{const} \quad (7)$$

The parameterization of the dielectric constant pretransitional effect via Eq. (5) is burdened with the necessity of using the multi-parameter nonlinear fitting routine. This problem can be reduced by introducing preliminary derivative-based and distortions-sensitive analysis, referenced to Eq. (5). Namely:

$$\frac{d\epsilon(P)}{dP} = a_p + A_p(1 - \alpha)(P^* - P)^{-\alpha} = -a_p + c(P^* - P)^{-1/2} \quad (8)$$

where  $c = A_p(1 - \alpha) = \text{const}$  and the exponent  $\alpha = 1/2$ .

Basing on the above relation, one can propose the following linearized scaling relation:

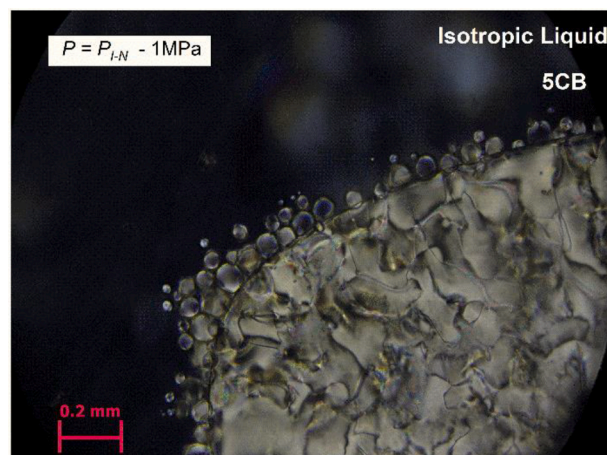


Fig. A3.1. Polarization microscopy insight into pentylcyanobiphenyl (5CB) on compressing: the isotropic liquid phase.

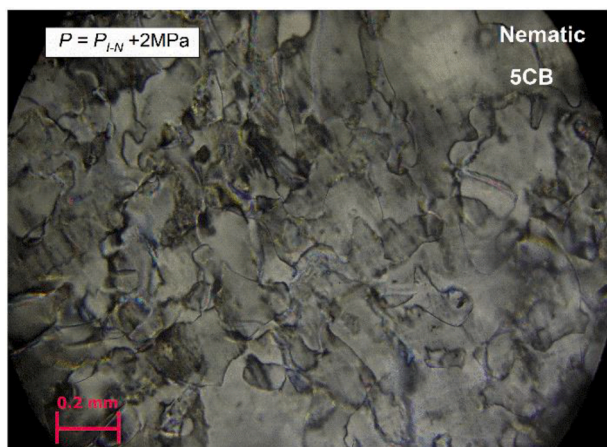


Fig. A3.2. Polarization microscopy insight into pentylcyanobiphenyl (5CB) on compressing: the nematic phase.

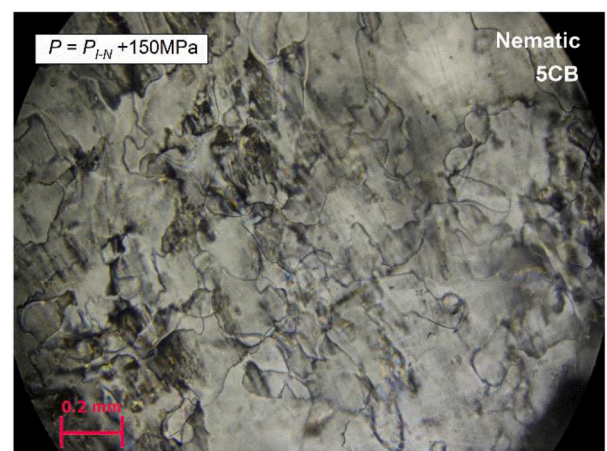


Fig. A3.3. Polarization microscopy insight into pentylcyanobiphenyl (5CB) on compressing: the nematic phase.

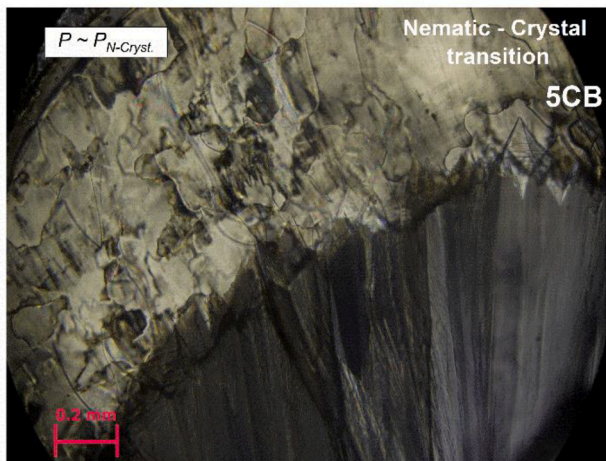


Fig. A3.4. Polarization microscopy insight into pentylcyanobiphenyl (5CB) on compressing: the nematic – crystal transition.

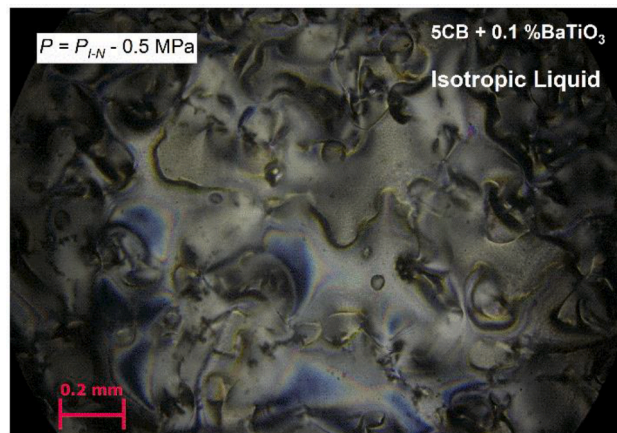


Fig. A3.7. Polarization microscopy insight into pentylcyanobiphenyl (5CB) and 0.1% of BaTiO<sub>3</sub> nanoparticles (2r = 50nm) on compressing: the isotropic liquid phase just above I-N transition.



Fig. A3.5. Polarization microscopy insight into pentylcyanobiphenyl (5CB) on compressing: the solid crystal phase.

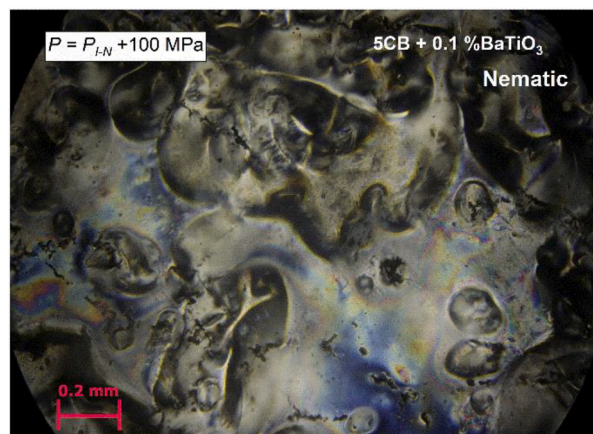


Fig. A3.8. Polarization microscopy insight into pentylcyanobiphenyl (5CB) and 0.1% of BaTiO<sub>3</sub> nanoparticles (2r = 50nm) on compressing: the nematic phase.

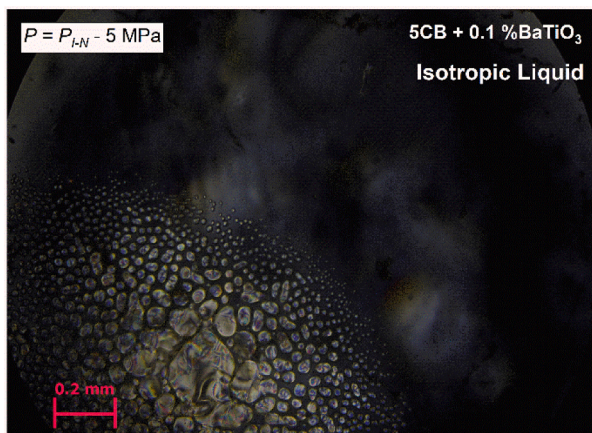


Fig. A3.6. Polarization microscopy insight into pentylcyanobiphenyl (5CB) and 0.1% of BaTiO<sub>3</sub> nanoparticles (2r = 50nm) on compressing: the isotropic liquid phase.

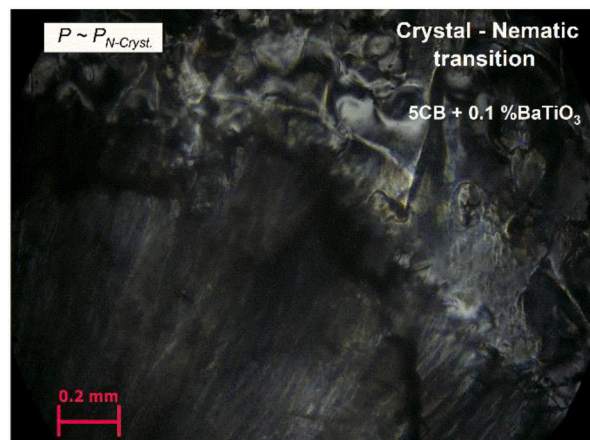


Fig. A3.9. Polarization microscopy insight into pentylcyanobiphenyl (5CB) and 0.1% of BaTiO<sub>3</sub> nanoparticles (2r = 50nm) on compressing: the nematic – crystal transition.

$$\left(\frac{\varepsilon(P)}{dP} + a_p\right)^{-2} = c^{-2}P^* - c^{-2}P \tag{9}$$



**Fig. A3.10.** Polarization microscopy insight into pentylcyanobiphenyl (5CB) and 0.1% of BaTiO<sub>3</sub> nanoparticles ( $2r = 50nm$ ) on compressing: the solid crystal phase.

where

$$c^{-2}P^* = const$$

Experimental  $\varepsilon(P)$  data can be preliminary analyzed via Eq. (9), using only a single adjustable parameter ( $a_p$ ). The linear behavior domain in the plot defined by Eq. (9) validates the description of the pretransitional effect by Eqs. (5) and (8). It is shown in Fig. 4. The subsequent linear regression fit yields optimal values of the relevant parameters. Worth stressing is the direct estimation of  $P^*$  and  $\Delta P^*$  values, as indicated in Fig. 4. The most striking feature of results presented in Figs. 3 and 4 is the near-continuous I-N transition, i.e. related to  $\Delta P^* \rightarrow 0$ , for a (very) minimal addition ( $x = 0.1\%$ ) of nanoparticles. When the amount of NPs increases to concentration  $x = 1\%$ , a significant discontinuity appears ( $\Delta P^* \approx 32MPa$ ), although it is lower than for pure 5CB:  $\Delta P^* \approx 82MPa$ .

In the nematic mesophase, LC samples are often ‘oriented’ for detecting separately parallel ( $\varepsilon_{||}$ ) and perpendicular ( $\varepsilon_{\perp}$ ) components of the dielectric constant, significant for rod-like molecules. They are associated with the rod-like or ellipsoidal symmetry of LC molecules. The basic way of LC nematic sample ordering is via using a strong magnetic field. This approach is not possible for high-pressure studies. The alternative experimental technique for the orientation of LC samples is related to covering capacitor plates with a polymeric agent supporting the required orientation of LC molecules. However, pressure can distort or even remove the layer, because of qualitatively different compressibilities of the ‘soft’ polymeric layer and the ‘hard’ metal electrodes. It resembles biofilm removal from a metal surface via compressing [64]. Such action of pressure can also introduce parasitic molecular impurities. It can essentially bias results because phase transition related phenomena in LC compounds are extremely sensitive to such factors [4,65-67]. This report is focused on bulk properties, in non-oriented samples on compressing.

Fig. 2 shows that in the nematic phase of pure 5CB and its  $x = 1\%$  nanocolloid dielectric constant strongly increases on moving away from the clearing point, which resembles the behavior observed for the ‘parallel’ oriented samples, i.e.,  $\varepsilon_{||}(P)$ . Dielectric constant increases up to  $\varepsilon \approx 18.3$  in pure 5CB and even  $\varepsilon \approx 20.9$  in the nanocolloid for  $P \approx 233MPa$ . The latter value is higher than ever observed for  $\varepsilon_{||}(T)$  studies in the nematic phase of 5CB. It cannot be explained by the contribution from nanoparticles: it is only  $x = 1\%$  of paraelectric BaTiO<sub>3</sub>.

Generally, isotropic squeezing of rod-like particles/molecules can lead to the total orientation of the whole sample if for the process onset even a local preference for a ‘parallel’ or ‘perpendicular’ arrangement

exists. It can be associated with interactions with the surface of the capacitor or fluctuations. The manifestation of such effects can be found in ref. [66] for instance. For the discussed nanocolloid, one can suppose that the extreme uniaxial ordering leading to a very large dielectric constant can result from the synergic impacts of compressing and BaTiO<sub>3</sub> nanoparticles influencing the orientation of the main part of 5CB molecules. Notable that the alkyl chain in n-cyanobiphenyls (nCB) molecules is slightly tilted relative to the direction of the main part of the molecule containing two phenyl rings. This causes that when using the magnetic field or electric field to align 5CB molecules in temperature studies under atmospheric pressure, the permanent dipole moment is inherently tilted with respect to the preferred direction, and only the dipole moment component related to the projection of it on the preferred direction determined by the external field is detected. Compressing can reduce this factor. In nanocolloids, adding some optimal amount of paraelectric BaTiO<sub>3</sub> may introduce further impact by minimizing the steric hindrance. For both pure 5CB and its  $x = 1\%$  nanocolloid dielectric constant first rises and subsequently significantly decreases when increasing pressure to values higher than  $P > 233MPa$  in the nematic phase. The question arises of the origins of such behavior. In refs. [36,37] high resolution  $\varepsilon_{||}(T)$  and  $\varepsilon_{\perp}(T)$  temperature studies under atmospheric pressure were carried out. These data were used for the analysis of order parameter  $\Delta\varepsilon_M(T) = \varepsilon_{||}(T) - \varepsilon_{\perp}(T)$  and diameter  $d(T) = (1/3)\varepsilon_{||}(T) + (2/3)\varepsilon_{\perp}(T)$  pretransitional changes in the nematic phase. These results are briefly recalled in Appendix 2, where also the relation for pretransitional changes of  $\varepsilon_{||}(T)$  and  $\varepsilon_{\perp}(T)$  separately is derived. Basing on the Isomorphism Postulate for Critical Phenomena [4] one can introduce the pressure counterpart for  $\varepsilon_{||}(P)$  changes in the nematic phase:

$$\varepsilon_{||}(P) = \varepsilon^{**} + B_P(P - P^{**})^{\beta} + A_P(P - P^{**})^{1-\alpha} + a_P(P - P^{**}) \quad (10)$$

To reduce the number of parameters, we implemented the effective critical exponent concept as in [57], for which the second power term in Eq (10) is considered as a weighted correction to the first, leading term:

$$\varepsilon_{||}(P) = \varepsilon^{**} + B_P(P - P^{**})^{\beta_{eff.}} + a_P(P - P^{**}) \quad (11)$$

The latter equation allows the reduction of parameters number, particularly important for nonlinear fitting. In Fig. 2 changes of dielectric constant in the nematic phase for pure 5CB and its  $x = 1\%$  NPs nanocolloid are well portrayed by Eq. (10), with the order parameter effective exponent  $\beta_{eff.} \approx 0.65$  which can indicate the reference value  $\beta = 1/2$ . This result shows that the bending down remote from I-N transition is the inherent feature of the I-N pretransitional behavior in the nematic phase, and should not be associated with approaching on compressing solid phase.

In temperature studies (under atmospheric pressure) most often constant and temperature-independent values of  $\varepsilon_{||}(T)$  and  $\varepsilon_{\perp}(T)$  are reported in the nematic phase, well below  $T_{I-N}$  [32]. These data are used for reliable estimations of dielectric constant anisotropy  $\Delta\varepsilon(T \ll T_{I-N}) = \varepsilon_{||} - \varepsilon_{\perp}$ . However, for a limited number of reports the ‘bending’ behavior is reported [68-70]. It takes place in LC systems, with the extended range of the nematic phase, for instance, due to supercooling shifting the N-Cr melting temperature, well below reference ‘equilibrium’ values. It is visible in Fig. 2 that when passing Nematic – Solid pressure on compressing dielectric constant strongly decreases. For 5CB + 0.1% BaTiO<sub>3</sub> nanocolloid it is  $\varepsilon \approx 2.2$ . Such value is typical for a crystalline phase with frozen orientational and translational freedom. However, for pure 5CB dielectric constant drops only to  $\varepsilon \approx 5.2$ , and for 5CB + 1% BaTiO<sub>3</sub> nanocolloid  $\varepsilon \approx 4.3$ . These relatively large values of dielectric constant can indicate the existence of the plastic crystalline phase, which was experimentally observed for a solidified nematic phase of rod-like LC molecules, although the crucial dielectric spectroscopy evidence is still lacking. The nature of this phase still constitutes a challenge. Notwithstanding, one can recall the model analysis by Onsager [71] regarding the onset of the crystalline state for the rod-like colloidal and molecular

system. He suggested the appearance of collisions on approaching the phase transitions, with the time scale faster than a ‘critical value’ necessary to maintain the orientational order. Following this, in the solid phase below the nematic phase, the appearance of the translational order matched with the high degree of the orientational disorder was suggested.

On decreasing frequency below the static domain (see Fig. 1), the strong rise of  $\epsilon'(f)$  takes place. It is associated with the increasing impact of the ionic-related, translational contribution to polarizability. This low-frequency domain is extensively tested due to its particular significance for practical applications. Notwithstanding, the impact of pretransitional fluctuations on dielectric properties in the LF domain remains puzzling in pure LC and its nanocolloids. To the best of the authors’ knowledge, only in refs. [72-74] for 5CB and 11CB it was shown that the ‘matrix’ created by the pretransitional fluctuations leads to linear changes of the ionic contribution to dielectric permittivity, namely:

$$\Delta\epsilon(f, T) = \epsilon'(f, T)_{LF} - \epsilon(T) = A(f) + B(f) \times T \quad (12)$$

where  $\epsilon(T)$  is the reference dielectric constant change determined for  $\epsilon'(T)$  in the static domain, and ‘‘LF’’ indicates frequencies in the low-frequency region.  $A(f), B(f)$  are constant parameters (for the given measurement frequency).

For the static domain, dielectric properties associated with the real part of dielectric permittivity are characterized by dielectric constant, i. e.,  $\epsilon = \epsilon'(T)$ . The main contribution to the dielectric constant in the tested system is associated with the permanent dipole moment. It is supplemented by a minor impact related to atomic and electronic polarizabilities. On decreasing frequency from the static domain, most often for  $f < 1\tilde{\text{A}}\cdot 10\text{kHz}$  the impact of low-frequency (LF) contributions appears and strongly increases values of  $\epsilon'(f)$ . This contribution is most often explained as the consequence of residual ionic contaminations. These features of dielectric permittivity spectra are shown in detail in Fig. 1. Consequently, Eq. (12) relates to the ‘extracted’, LF behavior. The linear evolution was evidenced in the isotropic liquid phase on approaching I-N transition.

Fig. 5 shows that similar behavior occurs for pressure-related behavior, namely:

$$\Delta\epsilon(f, P) = \epsilon'(f, P)_{LF} - \epsilon(T) = A(f) + B(f) \times P, \quad T = \text{const} \quad (13)$$

Notable that the most considerable impact of the ionic contribution takes place for  $x = 0.1\%$  BaTiO<sub>3</sub> nanocolloid, i.e., for the system showing the continuous I-N transition.

Fig. 6 presents the primary relaxation time as a function of pressure in the nematic phase of tested systems. Generally, for pressure-related changes in relaxation time, one can expect the description via the super-Barus (SB) relation [5,60,61]:

$$\tau(P) = \tau_0 \exp\left(\frac{PV_a(P)}{RT}\right) \quad (14)$$

where  $\tau_0 = \text{const.}$ ,  $V_a(P)$  is the apparent activation volume,  $R$  denotes the gas constant.

As visible in Fig. 5, remote from the I-N transition, the basic Barus relation with  $V_a(P) = V_a = \text{const}$  emerges. It is associated with the same activation volume  $V_a = 40\text{cm}^3/\text{mol}$  for each tested system. Strong, pretransitional distortions occur near the I-N transition, starting from  $P_{I-N} 160\text{MPa}$ . The impact of nanoparticles is here different than for dielectric constant. Namely  $\tau(P)$  changes in pure 5CB (discontinuous transition) and 5CB + 0.1% BaTiO<sub>3</sub> nanocolloids (continuous phase transition) follow the same track. Notably, the primary relaxation process is faster in pure 5CB than in related nanocolloids.

Fig. 7 focuses on discussing the distribution of relaxation times in the nematic phase of tested systems. It shows the Jonsher-type [75] normalized superposition of dielectric loss curves for 5CB and tested

nanocolloids, for the pressure in the mid of the nematic phase:

$$\epsilon''(f < f_{peak}) \propto \left(\frac{f}{f_{peak}}\right)^m, \quad \epsilon''(f > f_{peak}) \propto \left(\frac{f}{f_{peak}}\right)^{-n} \quad (15)$$

For comparison, the Debye curve [60] related to the single relaxation time and  $m = n = 1$  [68] is also plotted. For pure 5CB the broadening of the distributions of relaxation times, in comparison to the reference Debye curve, is visible, both for the low- ( $f < f_{max}$ ) and high- ( $f > f_{max}$ ) frequency parts. The addition of nanoparticles shifts the distribution towards the basic Debye pattern.

Studies of the evolution of the primary relaxation time are associated with the dynamics of orientational processes. Tests of DC electric conductivity contain a message related to the translational processes. In complex systems, both properties are often decoupled, which is expressed by the fractional Debye-Stokes-Einstein (fDSE) relation [76].

Fig. 8 shows its implementation for the pressure path, namely [76]:

$$\sigma(P)[\tau(P)]^S = C = \text{const} \Rightarrow \ln\sigma(P) = -S\ln\tau(P) + C \quad (16)$$

where  $T = \text{const}$  and the exponent  $S = 1$  is related to the translational-orientational coupling, i.e., to the basic reference DSE law.

Fig. 8 presents the explicit fDSE behavior in tested systems. Pure 5CB and its  $x = 1\%$  nanocolloid in the nematic phase show a similar degree of decoupling. It is notably smaller for  $x = 0.1\%$  nanocolloid. Significant hallmarks of phase transitions and pretransitional effects, strongly manifested in temperature studies under atmospheric pressure, are very limited in the reported pressure test. Furthermore, there might be several reasons for the weakening of the I-N phase transition for small concentrations of BaTiO<sub>3</sub>. The interlayer correlation can be reduced for a small concentration of NPs. In this case, the coupling between the orientational order parameter and nanoparticle order parameter decreases, resulting in such a weakening of the transition. A small concentration of the paraelectric BaTiO<sub>3</sub> reduces the pressure range of the nematic phase. The pressure range of hysteresis associated with the I-N transition becomes smaller when the pressure range of the nematic phase is reduced. Consequently, the I-N transition, which has a first-order character in bulk, changes to a continuous one for a small concentration of BaTiO<sub>3</sub> NPs. Owing to the restricted size of the nanoparticle to which the correlations can grow, the disorder is substantial at a small concentration of BaTiO<sub>3</sub>. The presence of disorder weakens the strength of the transition, causing the first-order character of the I-N transition to change to the continuous one.

#### 4. Conclusions

The report shows the first comprehensive test of static and dynamic dielectric properties in compressed rod-like nematogenic liquid crystalline compound (5CB) and its nanocolloids with BaTiO<sub>3</sub> nanoparticles. Studies extend from the low-frequency domain to the relaxation region, focusing on the impact of pretransitional fluctuations. The difference between temperature (T) and pressure (P) studies is worth stressing. In complex liquids and soft matter systems, where LC compounds and their nanocolloids can be encountered, cooling or heating can change the activation energy for processes. For compressing, the activation volume can change. Hence, the knowledge of physical properties evolutions along  $P\&T$  paths is essential for complete insight. On the other hand, pretransitional/precritical changes of physical properties should be described by isomorphic functional dependences for  $P$  &  $T$  paths, with the same values of critical exponents. This feature is known as the isomorphism postulate for critical phenomena. This unique universality for the so-called field variables near the critical point is well proved experimentally [4]. Griffiths and Wheeler [77] explained it theoretically by considering unique space features near the critical point. De Gennes indicated the meaning of  $\Delta T^*$  as the metric of the I-N transition discontinuity for rod-like molecules based liquid crystalline systems

[9,10]. It usually spans from ca. 0.8 K to 2 K. Compressing significantly increases  $\Delta T^*$ , as it is presented in Appendix 1 and ref. [78]. As shown in ref. [78] the isotropic stretching, i.e., negative pressures - the natural extension of compressing, can only slightly reduce  $\Delta T^*$ . Studies regarding the impact of nanoparticles on  $\Delta T^*$  in LC based systems are still very limited. They require precise tests of well-defined, from the point of critical phenomena physics, properties in an extended range of temperatures or pressure. Probably the first such studies were carried out only in the last years by the authors of this report. Some basic features of the phenomenon have to be recalled. First, adding nanoparticles to LC host, which can create a stable nanocolloidal system is possible only for a relatively small concentration of nanoparticles, namely  $x < 1\% \text{--} 2\%$ . For this domain, the addition of nanoparticles has a negligible impact on the isotropic-mesophase transition temperature (clearing temperature). Above this domain, adding a macromolecular surface agent for the space stabilization of nanoparticles is required [52]. For such 3-component systems, the increase of nanoparticles concentration, paralleled by the molecular surface agent concentration increase, and the decrease of the clearing temperature is observed.

Moreover, the biphasic domain between the isotropic liquid and nematic phase can appear. It can be explained by ‘free’ molecules contamination, even a tiny amount of it induces mentioned phenomena in LC systems. The rise of nanoparticles and surface agent concentrations can lead to the ‘temperature stretching’ of the isotropic liquid – LC mesophase, destroying the canonic discontinuous transition. This report focuses on the low concentration of nanoparticles domain, where the canonic feature of discontinuous/weakly discontinuous phase transition is preserved, and the unique impact of nanoparticles concentration on  $\Delta T^*$  value has been discovered. Such studies always require precise measurements of physical properties with well-defined precritical behavior in a wide range of temperatures or pressures. Studies reported in refs. [51,56,68] showed that the addition of paraelectric BaTiO<sub>3</sub> nanoparticles first causes some decrease in  $\Delta T^*$ , with the minimum near  $x \approx 0.5\%$  and the strong increase in  $\Delta T^*$  on further concentration rise. However, temperature studies of dielectric constant under atmospheric pressure in pentyloxycyanobiphenyl (5OCB) revealed an extraordinary decrease to  $\Delta T^* < 0.3\text{K}$  for the concentration  $x = 0.1\%$  [68]. Preliminary test for the I-N transition in 5CB related to temperature studies under atmospheric pressure yielded only a slight decrease of  $\Delta T^*$  for a similar concentration. The test on isothermal compressing revealed an unusually very strong decrease of  $\Delta P^*$ , the pressure counterpart of  $\Delta T^*$ . The obtained value  $\Delta P^* \approx 1\text{MPa}$ , can be estimated in the temperature scale using  $dT_{I-N}/dP$  value, given in Appendix 1:  $\Delta P^* \rightarrow \Delta T^* = dT^*/dP \Delta P^* = \frac{0.25\text{K}}{\text{MPa}} x 1\text{MPa} < 0.25\text{K}$ . One should note that in high-pressure studies, reliable measurements with a resolution below 1 MPa still constitute a challenge. Notable that for pure 5CB ( $x = 0$ ) the strong increase of  $\Delta P^*$  occurs, as generally expected for the I-N transition. Commenting on the above results, we would like to recall the conclusion of ref. [79], developed originally for the nematic transition in elastomeric soft materials ‘... weak random anisotropy results in a singular renormalization of the Landau-De Gennes expression, adding an energy term proportional to the inverse quartic power of order parameter  $Q$ . This reduces the first-order discontinuity ... For sufficiently high disorder strength the jump disappears altogether and the phase transition becomes continuous, in some ways

## Appendix 1

Compressing increases the clearing temperature and the related temperature of the hypothetical continuous phase transition.

In refs. [37,78] their portrayal via the following extension of the Simon-Glatzel dependence, introduced for describing pressure changes of the melting temperature, was proposed. For the I-N transition and the coupled continuous phase transition, it has the form [37]:

$$T_{I-N}(P), T^*(P) = T_{ref.} \left( 1 + \frac{\Delta P}{\Pi} \right)^{1/b} \exp \left( -\frac{\Delta P}{c} \right) = T_{ref.} \left( 1 + \frac{P - P_{ref.}}{\pi + P_{ref.}} \right)^{1/b} \exp \left( -\frac{P - P_{ref.}}{c} \right) \quad (\text{A1.1})$$

resembling the supercritical transitions in external field ...’ In this report it is shown that, the mentioned disorder can be introduced by the proper concentration of BaTiO<sub>3</sub> nanoparticles, which impact is additionally tuned by compressing. Notwithstanding, the common impact of nanoparticles and pressure on I-N transition requires further experimental, as well as, lacking so far, theoretical studies.

Notable is also the possibility of creating the ‘endogenic orientation’ by compressing matched with the addition of nanoparticles, leading to the enormous increase of dielectric constant.

Worth indicating the new explanation for the ‘bending’ behavior of the dielectric constant observed earlier in the test under atmospheric pressure for systems with a wide range of the nematic phase. The analysis in the given report links it to long-range consequences of the pretransitional behavior.

The synergic impact of nanoparticles and pressure on the nematic phase also led to the large ‘jump’ of dielectric constant at the nematic – solid (N-S) strongly discontinuous transition. Following refs. [80,81] such a change of dielectric constant can introduce a remarkable additional contribution to the phase transition entropy  $\Delta S_E \Delta \epsilon / T \approx 60\text{JK}^{-1}\text{kg}^{-1}$  supplementing the already large reference value recalled in the Introduction. Hence one can expect the colossal barocaloric effect [82,83]: in the given case 5CB and 5CB nanocolloids systems, are already at very moderate pressures. Notable is also the glassy dynamics detected in nematic 5CB and its nanocolloids, although the impact of pretransitional fluctuations under compression seems to be smaller than in reference temperature tests under atmospheric pressure.

### Experimental data availability

The author declares the availability of experimental data upon reasonable request.

### CRediT authorship contribution statement

**JŁ:** Formal Analysis, Investigation, Writing – original draft, Data curation. **ADR:** Formal Analysis, Writing – original draft, Supervision, Methodology. **SJR:** Writing – original draft, Methodology, Formal Analysis, Funding acquisition. **SS:** Writing – original draft, Funding acquisition. **KC:** Resources. **PKM:** Writing – review & editing.

### Declaration of Competing Interest

The authors declare that they have no known competing financial interests or personal relationships that could have appeared to influence the work reported in this paper.

### Data availability

Data will be made available on request.

### Acknowledgments

This work was supported by the National Science Center (NCN Poland), grant number: 2022/45/B/ ST5/04005, the project headed by Sylwester J. Rzoska.

S.S. was supported by the Slovenian Research Agency (ARRS), grants numbers: P2-0232, J2-4447, J3-3066, J3-2533, and J3-3074.

where  $(T_{ref}, P_{ref})$  are reference temperature and pressure related to the analysis onset,  $c$  is for the damping pressure coefficient,  $-\pi$  denotes the terminal negative pressure for  $P \rightarrow 0$ ,  $b$  is the amplitude related to the first derivative of the bulk modulus.

Fig. A1 presents pressure changes of  $T_{I-N}(P)$  and  $T^*(P)$  in pentylcyanobiphenyl. The plot has been prepared based on earlier studies of the authors, employing the low-frequency nonlinear dielectric effect (static, LF NDE). For this method data analysis may be reduced to the linear regression fit applied for NDE reciprocals. The plot also shows the path of studies applied in the given report and temperature dependences of  $T_{I-N}(P)$  and  $T^*(P)$  pressure-related derivatives, in the semi-log scale.

The curves describing experimental evolutions in Fig. A1 are related to following values of parameters:  $-\pi = -316\text{MPa}$ ,  $b = 1.96$ ,  $c = 4.0\text{GPa}$  for  $T_{I-N}(P)$ , and  $-\pi = -264\text{MPa}$ ,  $b = 2.30$ ,  $c = 3.0\text{GPa}$  for  $T^*(P)$ .

## Appendix 2

In refs. [36,37] dielectric constant was tested in the nematic phase of a rod-like LC compound, for a sample oriented by the strong magnetic field, in such a way that simultaneous collection of data for  $\epsilon_{||}(T)$  and  $\epsilon_{\perp}(T)$  components (with respect to the long molecular axis) was possible. The following portrayal of the order parameter  $\Delta\epsilon_M(T) = \epsilon_{||}(T) - \epsilon_{\perp}(T)$  and the ‘diameter’ is defined as  $d(T) = (1/3)\epsilon_{||}(T) + (2/3)\epsilon_{\perp}(T)$  was shown:

$$\Delta\epsilon_M(T) = \Delta\epsilon^{**} + B(T^{**} - T)^{\beta} \quad (\text{A2.1})$$

$$d(T) = \epsilon_d^{**} + a_d(T^{**} - T) + A_d(T^{**} - T)^{1-\alpha} \quad (\text{A2.2})$$

In refs. [4], for 8OCB and 5CB, basing on the above relations and the supplementary derivative-based analysis the following values of critical exponent were obtained:  $\alpha \approx 0.5$ , and  $\beta \approx 0.25$ , which coincides with the ‘hidden tricriticality’ picture of the I-N transition.

Linking Eqs. (A2.1) and (A2.2) one can obtain equations portraying separately  $\epsilon_{||}(T)$  and  $\epsilon_{\perp}(T)$  changes, namely:

$$\epsilon_{||}(T) = d + \frac{2}{3}\Delta\epsilon_M(T) = C + a_d(T^{**} - T) + A_d(T^{**} - T)^{1-\alpha} + \frac{2}{3}B(T^{**} - T)^{\beta} \quad (\text{A2.3})$$

$$\epsilon_{\perp}(T) = C' + a_d(T^{**} - T) + A_d(T^{**} - T)^{1-\alpha} - \frac{1}{3}B(T^{**} - T)^{\beta} \quad (\text{A2.4})$$

where constant terms  $C = \epsilon_d^{**} + \frac{2}{3}\Delta\epsilon^{**}$  and  $C' = \epsilon_d^{**} - \frac{1}{3}\Delta\epsilon^{**}$

In the above relations ‘two stars’ (\*\*) indicate the hypothetical continuous phase transition temperature determined on approaching I-N transition from the nematic phase side. It leads to the estimation of another discontinuity metric  $\Delta T^{**}$ . Notable, that the comparison of discontinuities  $\Delta T^{**}$  for  $T \rightarrow (\text{Nematic}) \rightarrow T_{I-N}$  and  $\Delta T^*$  for  $T_{I-N} \leftarrow (\text{Isotropic}) \leftarrow T$  paths shows that  $\Delta T^{**}/\Delta T^* \approx 1/2$ . [37].

Following the Isomorphism Postulate for critical phenomena, parallel functional dependences describing pretransitional changes - with the same values of critical exponents - are expected for any field-variable-related path of approaching the critical point. Consequently, one can expect obeying pressure-related counterparts of Eqs. (A2.1 – A2.4). However, in the given case the experimental validation possibilities are very limited and require the development of experimental implementations.

## Appendix 3

Polarization microscopy photos for 5CB and 5CB + 0.1% BaTiO<sub>3</sub> nanocolloid on isothermal compressing ( $T = 353.0\text{K}$ ) are presented below. They reveal a notable impact of nanoparticles, despite their minimum amount (see Figs. A3.1-A3.10).

## References

- [1] Y. Suzuki, Direct observation of reversible liquid–liquid transition in a trehalose aqueous solution, PNAS 119 (2022), e2113411119, <https://doi.org/10.1073/pnas.2113411119>.
- [2] H. Tanaka, Liquid–liquid transition and polyamorphism, J. Chem. Phys. 153 (13) (2020) 130901, <https://doi.org/10.1063/5.0021045>.
- [3] M. Mierzwa, M. Paluch, S.J. Rzoska, J. Ziolo, The liquid–glass and liquid–liquid transitions of TPP at elevated pressure, J. Phys. Chem. B 112 (2008) 10383–10385, <https://doi.org/10.1021/jp8042158>.
- [4] M.A. Anisimov, Critical Phenomena in Liquids and Liquid Crystals, Gordon and Breach, Reading, 1992. ISBN: 9782881248061.
- [5] S.J. Rzoska, V. Mazur, A. Drozd-Rzoska (Eds.), Metastable Systems under Pressure, Springer Verlag, Berlin, 2010. ISBN: 9789048134076.
- [6] P. Collings, J.W. Goodby, Introduction to Liquid Crystals: Chemistry and Physics, CRC Press, Routledge (2019), <https://doi.org/10.1201/9781315272801>.
- [7] G.A. Oweimreen, M.A. Morsy, DSC studies on p-(n-alkyl)-p-cyanobiphenyl (RCB’s) and p-(n-alkoxy)-p-cyanobiphenyl (ROCB’s) liquid crystals, Thermochim. Acta 346 (2000) 37–47, [https://doi.org/10.1016/S0040-6031\(99\)00411-6](https://doi.org/10.1016/S0040-6031(99)00411-6).
- [8] Studies of the Authors of the given report.
- [9] P.G. de Gennes, Phenomenology of short-range order effects in the isotropic phase of nematic materials, Ph. ys. Lett. A 30 (1969) 454–455, [https://doi.org/10.1016/0375-9601\(69\)90240-0](https://doi.org/10.1016/0375-9601(69)90240-0).
- [10] P.G. de Gennes, Short-range order effects in the isotropic phase of nematic and cholesteric, Mol. Cryst. Liq. Cryst. 12 (1971) 193–214, <https://doi.org/10.1080/15421407108082773>.
- [11] T.W. Stinson, J.D. Litster, Pretransitional phenomena in the isotropic phase of a nematic liquid crystal, Phys. Rev. Lett. 25 (1970) 503–508, <https://doi.org/10.1103/PhysRevLett.25.503>.
- [12] J. Filippini, Y. Poggi, Kerr effect in the isotropic phase of nematic liquid crystals, J. Physique Lett. 35 (1974) 99–101, <https://doi.org/10.1051/jphyslet:01974003507-809900>.
- [13] J. Bendler, Compressibility and thermal expansion anomalies in the isotropic liquid crystal phase, Mol. Cryst. Liq. Cryst. 38 (1977) 19–30, <https://doi.org/10.1080/15421407708084371>.
- [14] K.-I. Muta, H. Takezoe, A. Fukuda, E. Kuze, Cotton-Mouton effect of alkyl- and alkoxy- cyanobiphenyls in isotropic phase, Jpn. J. Appl. Phys. 18 (11) (1979) 2073–2080.
- [15] V.N. Tsvetkov, E.I. Ryumtsev, Liquid Crystals, Kerr-effect in the isotropic liquid phase of nematogens, Mol. Cryst. Liq. Cryst. 133 (1986) 125–134, <https://doi.org/10.1080/00268948608079566>.
- [16] A. Drozd-Rzoska, S.J. Rzoska, J. Ziolo, Mean-field behaviour of the low frequency non-linear dielectric effect in the isotropic phase of nematic and smectic n-alkylcyanobiphenyls, Liquid Crystals 21 (1996) 273–277, <https://doi.org/10.1080/02678299608032833>.
- [17] A. Drozd-Rzoska, S.J. Rzoska, J. Ziolo, High-pressure studies of the low-frequency nonlinear dielectric effect in the isotropic phase of octyl- and dodecylcyanobiphenyls Phys. Rev. E 55 (3) (1997) 2888–2891.
- [18] A. Drozd-Rzoska, Influence of measurement frequency on the pretransitional behaviour of the non-linear dielectric effect in the isotropic phase of liquid crystalline materials, Liquid Crystals 24 (1998) 835–840, <https://doi.org/10.1080/026782998206650>.
- [19] A. Drozd-Rzoska, S.J. Rzoska, Complex relaxation in the isotropic phase of n-pentylcyanobiphenyl in linear and nonlinear dielectric studies, Phys. Rev. E 65 (2002) 2885–2889, <https://doi.org/10.1103/PhysRevE.65.041701>.

- [20] A. Ranjesh, S. Kiani, M.H. Parast, M.S. Zkerhamidi, T.-H. Yoon, Characterization of short-range molecular interaction by empirical solvent polarity scale to analyze the Kerr effect of nematic liquid crystals in the isotropic phase, *J. Mol. Liq.* 295 (2019), 111653, <https://doi.org/10.1016/j.molliq.2019.111653>.
- [21] L.D. Landau, E.M. Lifshitz, *Statistical Physics*, Pergamon, Oxford, 1958.
- [22] V. Zvetkoff, Über die molekülanordnung in der anisotropie-flüssigen phase, *Acta Physicochim. URSS* 16 (1942) 132–147.
- [23] V. Zvetkov, Magnetic and dynamic double refraction in the isotropic phase of substance capable of forming liquid crystals, *Acta Physicochim. URSS* 19 (1944) 86–103.
- [24] P.G. de Gennes, J. Prost, *The Physics of Liquid Crystals*, Oxford Univ. Press, Oxford, 1995.
- [25] R.J.A. Tough, M.J. Bradshaw, The determination of the order parameters of nematic liquid crystals by mean field extrapolation, *J. Physique* 44 (1983) 447–454, <https://doi.org/10.1051/jphys:01983004403044700>.
- [26] W. Gelbart, B. Barbo, A van der Waals picture of the isotropic-nematic liquid crystal phase transition, *Acc. Chem. Res.* 13 (1980) 290–296, <https://doi.org/10.1021/ar50152a007>.
- [27] J.M. Ball, A. Majumdar, Nematic liquid crystals: From Maier-Saupe to a continuum theory, *Mol. Cryst. Liq. Cryst.* 525 (2010) 2010–2016, <https://doi.org/10.1080/15421401003795555>.
- [28] D. Izo, M.J. de Oliveira, Landau theory for isotropic, nematic, smectic-A, and smectic-C phases, *Liquid Crystals* 47 (2019) 99–105, <https://doi.org/10.1080/02678292.2019.1631968>.
- [29] B. van Roie, J. Leys, K. Denolf, C. Glorieux, G. Pitsi, J. Thoen, Weakly first-order character of the nematic-isotropic phase transition in liquid crystals, *Phys. Rev. E* 72 (2005), 041702, <https://doi.org/10.1103/PhysRevE.72.041702>.
- [30] P.K. Mukherjee, The puzzle of the nematic-isotropic phase transition, *J. Phys.: Condens. Matter* 10 (1998) 9191–9201. The puzzle of the nematic-isotropic phase transition 1998 10.1088/0953-8984/10/41/003.
- [31] C. Vitoriano, Inclusion of mass density fluctuations in the Landau-de Gennes theory of nematic-isotropic phase transition, Brazil, *J. Phys.* 50 (2020) 24–28, <https://doi.org/10.1007/s13538-019-00725-x>.
- [32] D. Demus, J. Goodby, G.W. Gray, H.-W. Spiess, V. Vill, *Handbook of Liquid Crystals: Fundamentals*, Wiley-VCH, Weinheim, Germany, 1998.
- [33] M. Simões, D.S. Simeão, Corresponding states of order parameter in nematic liquid crystals, *Phys. Rev. E* 74 (2006), 051701, <https://doi.org/10.1103/PhysRevE.74.051701>.
- [34] D.D. Luders, D.A. Oliveira, N.M. Kimura, M. Simões, A.J. Palangana, Order parameter in the nematic-isotropic phase transition, *J. Mol. Liq.* 207 (2015) 195–199, <https://doi.org/10.1016/j.molliq.2015.03.005>.
- [35] S.J. Rzoska, J. Ziolo, W. Sulkowski, J. Jadżyn, G. Czechowski, Fluidlike behavior of dielectric permittivity in a wide range of temperature above and below the nematic-isotropic transition, *Phys. Rev. E* 64 (5) (2001), 052701, <https://doi.org/10.1103/PhysRevE.64.052701>.
- [36] S.J. Rzoska, A. Drozd-Rzoska, P.K. Mukherjee, D.O. Lopez, J.C. Martinez-Garcia, Distortions-sensitive analysis of pretransitional behavior in n-octyloxycyanobiphenyl (8OCB), *J. Phys. Cond. Matter* 25 (2013), 245105, <https://doi.org/10.1088/0953-8984/25/24/245105>.
- [37] A. Drozd-Rzoska, ‘Quasi-tricritical’ and glassy dielectric properties of a nematic liquid crystalline material, *Crystals* 10 (2020) 297, <https://doi.org/10.3390/cryst10040297>.
- [38] K. Takatoh, M. Sakamoto, R. Hasegawa, M. Koden, N. Itoh, M. Hasegawa (Eds.), *Alignment Technology and Applications of Liquid Crystal Devices*, CRC Press, Routledge, USA, 2019.
- [39] L. Mistura, Behavior of the dielectric constant near a critical point in fluid systems, *J. Chem. Phys.* 59 (1973) 4563–4564, <https://doi.org/10.1063/1.1680657>.
- [40] A. Drozd-Rzoska, S.J. Rzoska, High-pressure behavior of dielectric constant in a binary critical mixture, *Phys. Rev. E* 102 (2020), 042610, <https://doi.org/10.1103/PhysRevE.102.042610>.
- [41] J. Thoen, G. Menu, Temperature dependence of the static relative permittivity of octylcyanobiphenyl (8CB), *Mol. Cryst. Liq. Cryst.* 07 (1983) 163–176, <https://doi.org/10.1080/00268948308073148>.
- [42] A. Drozd-Rzoska, S.J. Rzoska, J. Ziolo, Critical behaviour of dielectric permittivity in the isotropic phase of nematogens, *Phys. Rev. E* 54 (1996) 6452–6456, <https://doi.org/10.1103/PhysRevE.54.6452>.
- [43] J. Viamontes, J.X. Tang, Continuous isotropic-nematic liquid crystalline transition of F-actin solutions, *Phys. Rev. E* 67 (2003), 040701, <https://doi.org/10.1103/PhysRevE.67.040701>.
- [44] S.K. Al-Zangana, M. Iluit, G. Boran, M. Turner, A. Viayaraghavan, I. Dirking, Dielectric spectroscopy of isotropic liquids and liquid crystal phases with dispersed graphene oxide, *Sci. Rep.* 6 (2016) 31885, <https://doi.org/10.1038/srep31885>.
- [45] D. Vigolo, J. Zhao, S. Handschin, X. Cao, A.J. deMello, R. Mezzenga, Continuous isotropic-nematic transition in amyloid fibril suspensions driven by thermophoresis, *Sci. Rep.* 7 (2017) 1211, <https://doi.org/10.1038/s41598-017-01287-1>.
- [46] S. Mishra, V. Manjuladevi, R. Gupta, S. Kumar, Experimental evidence of continuous isotropic-nematic phase transition in CdS nanowire nanocomposites of a nematic liquid crystal, *Liquid Crystals* 48 (2020) 1–11, <https://doi.org/10.1080/02678292.2020.1849833>.
- [47] M. Letz, R. Schilling, A. Latz, Ideal glass transitions for hard ellipsoids, *Phys. Rev. E* 62 (2000) 5173–5174, <https://doi.org/10.1103/PhysRevE.62.5173>.
- [48] T. Theenhaus, M.P. Allen, M. Letz, A. Latz, R. Schilling, Dynamical precursor of nematic order in a dense fluid of hard ellipsoids of revolution, *Eur. Phys. J. E: Soft Matter Biol. Phys.* 8 (2002) 269–274, <https://doi.org/10.1140/epje/i2001-10093-7>.
- [49] D. Chakrabarti, B. Bagchi, Glassiness of thermotropic liquid crystals across the isotropic–nematic transition, *Phys. Chem. B* 111 (2007) 11646–11657, <https://doi.org/10.1021/jp079516w>.
- [50] S.J. Rzoska, S. Starzonek, J. Łoś, A. Drozd-Rzoska, S. Kralj, Dynamics and pretransitional effects in C<sub>60</sub> fullerene nanoparticles and liquid crystalline dodecylcyanobiphenyl (12CB) hybrid system, *Nanomaterials* 10 (2020) 2343, <https://doi.org/10.3390/nano10122343>.
- [51] J. Łoś, A. Drozd-Rzoska, S.J. Rzoska, S. Starzonek, K. Czupryński, Fluctuations-driven dielectric properties of liquid crystalline octyloxycyanobiphenyl and its nanocolloids, *Soft Matter* 18 (2022) 4502–4512, <https://doi.org/10.1039/D2SM00105E>.
- [52] J.P.F. Lagerwall, *Liquid Crystals with Nano and Microparticles*. World Sci. Pub., Singapore, 2016. <https://doi.org/10.1142/9280>.
- [53] I. Dierking, *Nanomaterials in Liquid Crystals*. MDPI, Basel, Switzerland, 2018, <https://doi.org/10.3390/nano8070453>.
- [54] S. Thomas, N. Kalarikkal, A.R. Abraham (Eds.), *Fundamentals and Properties of Multifunctional Nanomaterials (Micro and Nano Technologies)*, Elsevier, Amsterdam, Netherlands, 2021.
- [55] Barium Titanate BaTiO<sub>3</sub> Nanoparticles / Nanopowder (BaTiO<sub>3</sub>, 99.9%, 50nm, Cubic). <https://www.us-nano.com/inc/sdetail/532> (accessed 2021-01-19).
- [56] A. Drozd-Rzoska, S. Starzonek, S.J. Rzoska, S. Kralj, Nanoparticle-controlled glassy dynamics in nematogen-based nanocolloids, *Phys. Rev. E* 99 (2019), 052703, <https://doi.org/10.1103/PhysRevE.99.052703>.
- [57] A. Drozd-Rzoska, S.J. Rzoska, J. Kalabiński, The impact of pressure on low molecular weight near-critical mixtures of limited miscibility, *ACS Omega* 5 (2020) 20141–20152, <https://doi.org/10.1021/acsomega.0c01772>.
- [58] F. Schönhal, A. Kremer, *Broadband Dielectric Spectroscopy*, Springer, Berlin, Germany, 2003.
- [59] A. Drozd-Rzoska, Universal behavior of the apparent fragility in ultraslow glass forming systems, *Sci. Rep.* 9 (2019) 6816, <https://doi.org/10.1038/s41598-019-42927-y>.
- [60] A. Drozd-Rzoska, Pressure-related universal behavior of the structural relaxation time and apparent fragility, *Front. Mater.* 6 (2019) 103, <https://doi.org/10.3389/fmats.2019.00103>.
- [61] A. Drozd-Rzoska, Activation volume in superpressed glassformers, *Sci. Rep.* 9 (2019) 13787, <https://doi.org/10.1038/s41598-019-49848-w>.
- [62] P. Habdas, M. Paluch, A. Drozd-Rzoska, P. Malik, S.J. Rzoska, Pressure and temperature studies of dielectric permittivity in the homogeneous phase of nitrobenzene-dodecane binary mixture, *Chem. Phys.* 241 (3) (1999) 351–357.
- [63] S.J. Rzoska, P. Urbanowicz, A. Drozd-Rzoska, M. Paluch, P. Habdas, Pressure behaviour of dielectric permittivity on approaching the critical consolute point, *Europhys. Lett.* 45 (1999) 334–340, <https://doi.org/10.1209/epl/1999-00168-7>.
- [64] S.J. Rzoska and A. Drozd-Rzoska (inventors), patent application IHPP PAS submitted to the Patent Office Republic of Poland (2022).
- [65] S.J. Rzoska, J. Ziolo, The nonlinear dielectric effect applied to study the pretransitional effects in the isotropic phase of the MBBA - benzene solutions, *Acta Phys. Polon. A* 78 (1990) 915–919.
- [66] S.J. Rzoska, J. Ziolo, Critical properties in the vicinity of the critical consolute point for the 4-methoxybenzylidene-4-butylaniline - isooctane solution, *Liquid Crystals* 11 (1992) 9–14, <https://doi.org/10.1080/02678299208028964>.
- [67] J. Kalabiński, A. Drozd-Rzoska, S.J. Rzoska, phase equilibria and critical behavior in nematogenic MBBA-isooctane monotectic-type mixtures, *Int. J. Mol. Sci.* 24 (3) (2023) 2065.
- [68] S. Starzonek, S.J. Rzoska, A. Drozd-Rzoska, K. Czupryński, S. Kralj, Impact of ferroelectric and superparaelectric nanoparticles on phase transitions and dynamics in nematic liquid crystals, *Phys. Rev. E* 96 (2017), 022705, <https://doi.org/10.1103/PhysRevE.96.022705>.
- [69] N. Trbojevic, D.J. Read, M. Nagaraj, Dielectric properties of liquid crystalline dimer mixtures exhibiting the nematic and twist-bend nematic phases, *Phys. Rev. E* 96 (2017), 052703, <https://doi.org/10.1103/PhysRevE.96.052703>.
- [70] P. Sreenilayam, N. Yadav, Y.P. Panarin, G. Shanker, J.K. Vij, Electrooptic, pyroelectric and dielectric spectroscopic studies of nematic and twist bend nematic phases of achiral hockey-shaped bent-core liquid crystal, *J. Mol. Liq.* 351 (2022), 118632, <https://doi.org/10.1016/j.molliq.2022.118632>.
- [71] L. Onsager, The Effects of Shape on the Interaction of Colloidal Particles, *Ann. NY. Acad. Sci.* 51 (1949) 621–659, <https://doi.org/10.1111/j.1749-6632.1949.tb27296.x>.
- [72] A. Drozd-Rzoska, S.J. Rzoska, J. Ziolo, J. Jadżyn, Quasi-critical behavior of the low-frequency dielectric permittivity in the isotropic phase of n-pentylcyanobiphenyl, *Phys. Rev. E* 63 (2001) 052701–052704, <https://doi.org/10.1103/PhysRevE.63.052701>.
- [73] J. Łoś, A. Drozd-Rzoska, S.J. Rzoska, K. Czupryński, The impact of ionic contribution to dielectric permittivity in 11CB liquid crystal and its colloids with BaTiO<sub>3</sub> nanoparticles, *Eur. Phys. J. E* 45 (2022) 74, <https://doi.org/10.1140/epje/s10189-022-00228-9>.
- [74] J. Łoś, A. Drozd-Rzoska, S.J. Rzoska, Critical-like behavior of low-frequency dielectric properties in compressed liquid crystalline octyloxycyanobiphenyl (8OCB) and its nanocolloid with paraelectric BaTiO<sub>3</sub>, *J. Mol. Liq.* 377 (2023), 121555, <https://doi.org/10.1016/j.molliq.2023.121555>.
- [75] A.K. Jonscher, The ‘universal’ dielectric response, *Nature* 267 (1977) 673–679, <https://doi.org/10.1038/267673a0>.
- [76] S. Starzonek, S.J. Rzoska, A. Drozd-Rzoska, S. Pawlus, E. Biała, J.C. Martinez-Garcia, L. Kistersky, Fractional Debye–Stokes–Einstein behaviour in an ultraviscous nanocolloid: glycerol and silver nanoparticles, *Soft Matter* 11 (27) (2015) 5554–5562.

- [77] R.B. Griffiths, J.C. Wheeler, Critical points in multicomponent systems, *Phys. Rev. A* 2 (1970) 1047–1064, <https://doi.org/10.1103/PhysRevA.2.1047>.
- [78] S.J. Rzoska, P.K. Mukherjee, M. Rutkowska, Does the characteristic value of the discontinuity of the isotropic–mesophase transition in n-cyanobiphenyls exist? *J. Phys. Condens. Matt.* 24 (37) (2012) 375101, <https://doi.org/10.1088/0953-8984/24/37/375101>.
- [79] L. Petridis, E.M. Terentjev, Nematic-isotropic transition with quenched disorder *Phys. Rev. E* 74 (2006), 051707, <https://doi.org/10.1103/PhysRevE.74.051707>.
- [80] S.J. Burns, Linear dielectric thermodynamics: A new universal law for optical, dielectric constants, *J. Am. Ceram. Soc.* 104 (2020) 2087–2101, <https://doi.org/10.1111/jace.17594>.
- [81] J. Parravicini, G. Parravicini, Measuring state-of-order by dielectric response: a comprehensive review on Fröhlich entropy estimation, *Results in Physics* 28 (2021), 104571, <https://doi.org/10.1016/j.rinp.2021.104571>.
- [82] P. Lloveras, A. Aznar, M. Barrio, P.h. Negrier, C. Popescu, A. Planes, L. Mañosa, E. Stern-Taulats, A. Avramenko, N.D. Mathur, X. Moya, J.-Ll. Tamarit, Colossal barocaloric effects near room temperature in plastic crystals of neopentylglycol, *Nat. Comm.* 10 (2019) 1803, <https://doi.org/10.1038/s41467-019-09730-9>.
- [83] B. Li, Y. Kawakita, S. Ohira-Kawamura, T. Sugahara, H. Wang, J. Wang, Y. Chen, S. I. Kawaguchi, S. Kawaguchi, K. Ohara, K. Li, D. Yu, R. Mole, T. Hattori, T. Kikuchi, S.-I. Yano, Z. Zhang, Z. Zhang, W. Ren, S. Lin, O. Sakata, K. Nakajima, Z. Zhang, Colossal barocaloric effects in plastic crystals, *Nature* 567 (7749) (2019) 506–510, <https://doi.org/10.1038/s41586-019-1042-5>.